

## THEORETICAL STRESS-STRAIN MODEL FOR CONFINED CONCRETE

By J. B. Mander,<sup>1</sup> M. J. N. Priestley,<sup>2</sup> and R. Park,<sup>3</sup> Fellow, ASCE

**ABSTRACT:** A stress-strain model is developed for concrete subjected to uniaxial compressive loading and confined by transverse reinforcement. The concrete section may contain any general type of confining steel: either spiral or circular hoops; or rectangular hoops with or without supplementary cross ties. These cross ties can have either equal or unequal confining stresses along each of the transverse axes. A single equation is used for the stress-strain equation. The model allows for cyclic loading and includes the effect of strain rate. The influence of various types of confinement is taken into account by defining an effective lateral confining stress, which is dependent on the configuration of the transverse and longitudinal reinforcement. An energy balance approach is used to predict the longitudinal compressive strain in the concrete corresponding to first fracture of the transverse reinforcement by equating the strain energy capacity of the transverse reinforcement to the strain energy stored in the concrete as a result of the confinement.

### INTRODUCTION

In the seismic design of reinforced concrete columns of building and bridge substructures, the potential plastic hinge regions need to be carefully detailed for ductility in order to ensure that the shaking from large earthquakes will not cause collapse. Adequate ductility of members of reinforced concrete frames is also necessary to ensure that moment redistribution can occur. The most important design consideration for ductility in plastic hinge regions of reinforced concrete columns is the provision of sufficient transverse reinforcement in the form of spirals or circular hoops or of rectangular arrangements of steel, in order to confine the compressed concrete, to prevent buckling of the longitudinal bars, and to prevent shear failure. Anchorage failure of all reinforcement must also be prevented.

Tests have shown that the confinement of concrete by suitable arrangements of transverse reinforcement results in a significant increase in both the strength and the ductility of compressed concrete. In particular, the strength enhancement from confinement and the slope of the descending branch of the concrete stress-strain curve have a considerable influence on the flexural strength and ductility of reinforced concrete columns.

Theoretical moment-curvature analysis for reinforced concrete columns, indicating the available flexural strength and ductility, can be

<sup>1</sup>Visiting Asst. Prof. of Civ. Engrg., State Univ. of New York at Buffalo, Buffalo, NY 14260.

<sup>2</sup>Prof. of Struct. Engrg., Univ. of California, San Diego, CA 92037.

<sup>3</sup>Prof. and Head of Civ. Engrg., Univ. of Canterbury, Christchurch, New Zealand.

Note. Discussion open until January 1, 1989. Separate discussions should be submitted for the individual papers in this symposium. To extend the closing date one month, a written request must be filed with the ASCE Manager of Journals. The manuscript for this paper was submitted for review and possible publication on December 30, 1986. This paper is part of the *Journal of Structural Engineering*, Vol. 114, No. 8, August, 1988. ©ASCE, ISSN 0733-9445/88/0008-1804/\$1.00 + \$.15 per Paper No. 22686.

conducted providing the stress-strain relation for the concrete and steel are known. The moments and curvatures associated with increasing flexural deformations of the column may be computed for various column axial loads by incrementing the curvature and satisfying the requirements of strain compatibility and equilibrium of forces. The cover concrete will be unconfined and will eventually become ineffective after the compressive strength is attained, but the core concrete will continue to carry stress at high strains. The compressive stress distributions for the core and cover concrete will be as given by the confined and unconfined concrete stress-strain relations. Good confinement of the core concrete is essential if the column is to have a reasonable plastic rotational capacity to maintain flexural strength as high curvatures. In general, the higher the axial compressive load on the column, the greater the amount of confining reinforcement necessary to achieve ductile performance. This is because a high axial load means a large neutral axis depth, which in turn means that the flexural capacity of the column is more dependent on the contribution of the concrete compressive stress distribution.

Clearly it is important to have accurate information concerning the complete stress-strain curve of confined concrete in order to conduct reliable moment-curvature analysis to assess the ductility available from columns with various arrangements of transverse reinforcement.

In this paper, a unified stress-strain model for confined concrete is developed for members with either circular or rectangular sections, under static or dynamic loading, either monotonically or cyclically applied. The concrete section may contain any general type of confinement with either spirals or circular hoops, or rectangular hoops with or without supplementary cross ties, with either equal or unequal confining stresses along each of the transverse axes. The model includes the effects of cyclic loading and strain rate. Full details of the proposed model is discussed elsewhere (Mander et al. 1984).

In a companion paper by Mander et al. (1988), the theoretical model presented herein is compared with the results of an experimental program of some 40 concentric axial compression tests. This program consisted of nearly full-size circular, square, and rectangular reinforced concrete columns tested at either slow or fast (dynamic) rates of strain, with or without cyclic loading.

### PAST INVESTIGATIONS OF THE BEHAVIOR AND MODELING OF CONFINED CONCRETE

Early investigators showed that the strength and the corresponding longitudinal strain at the strength of concrete confined by an active hydrostatic fluid pressure can be represented by the following simple relationships:

$$f'_{cc} = f'_{co} + k_1 f_l \dots \dots \dots (1)$$

$$\epsilon_{cc} = \epsilon_{co} \left( 1 + k_2 \frac{f_l}{f'_{co}} \right) \dots \dots \dots (2)$$

where  $f'_{cc}$  and  $\epsilon_{cc}$  = the maximum concrete stress and the corresponding strain, respectively, under the lateral fluid pressure  $f_l$ ;  $f'_{co}$  and  $\epsilon_{co}$  =

unconfined concrete strength and corresponding strain, respectively; and  $k_1$  and  $k_2$  = coefficients that are functions of the concrete mix and the lateral pressure.

Richart et al. (1928) found the average values of the coefficients for the tests they conducted to be  $k_1 = 4.1$  and  $k_2 = 5k_1$ . Also, Balmer (1949) found from his tests that  $k_1$  varied between 4.5 and 7.0 with an average value of 5.6, the higher values occurring at the lower lateral pressures. Richart et al. (1929) also found that the strength of concrete with active confinement from lateral (fluid) pressure was approximately the same as for concrete with passive confinement pressure from closely spaced circular steel spirals causing an equivalent lateral pressure.

Different investigators, such as Mander et al. (1984), Scott et al. (1982), Sheikh and Uzumeri (1980), and Vellenas et al. (1977), have carried out numerous tests on nearly full-size specimens and have demonstrated that confinement is improved if (1) The transverse reinforcement is placed at relatively close spacing; (2) additional supplementary overlapping hoops or cross ties with several legs crossing the section are included; (3) the longitudinal bars are well distributed around the perimeter; (4) the volume of transverse reinforcement to the volume of the concrete core or the yield strength of the transverse reinforcement is increased; and (5) spirals or circular hoops are used instead of rectangular hoops and supplementary cross ties. Clearly it is important to be able to quantify these effects of confinement on the stress-strain behavior of concrete.

The complex endochronic mathematical model developed by Bazant and Bhat (1976, 1977) appears to be the only constitutive model that describes the stress-strain response under monotonic, cyclic, and dynamic loadings of confined or unconfined concrete with any state of multiaxial stress. However, endochronic constitutive models were developed using data based primarily on biaxial and triaxial tests with active confinement provided by mechanical means. Therefore, at this state of development, no rational allowance can be made for the passive confinement from the many different configurations of transverse reinforcement that are possible using various hoop shapes and spacings.

Early research on confined reinforced concrete behavior was generally carried out on small-scale concentrically loaded specimens at quasi-static rates of strain. The stress-strain model of Kent and Park (1971) for concrete confined by rectangular transverse reinforcement was based on the test results of Roy and Sozen (1964) and others available at that time. This early model neglected the increase in concrete strength but took into account the increase in ductility due to rectangular confining steel. More recently, Scott et al. (1982) and Park et al. (1982) have tested near full-size specimens based on real building columns and modified the Kent and Park (1971) stress-strain equations to take into account the enhancement of both the concrete strength and ductility due to confinement and the effect of strain rate. Monotonic stress-strain equations for concrete confined by rectangular-shaped transverse reinforcement include those proposed by Vellenas et al. (1977) and Sheikh and Uzumeri (1980). Stress-strain equations for concrete confined by spiral reinforcement have been proposed by Park and Leslie (1977), Desayi et al. (1978), Ahmad and Shah (1982, 1985), Dilger et al. (1984), and others.

The flexural strength and ductility of confined reinforced concrete

sections computed using those stress-strain equations show differences. In particular, the equations are grouped into those applicable to rectangular-shaped confining steel and those applicable to circular-shaped confining steel. It is evident that a unified approach applicable to all configurations of circular- and rectangular-shaped transverse reinforcement, and including the effects of cyclic loading and strain rate, is required.

**UNIFIED STRESS-STRAIN APPROACH FOR CONFINED CONCRETE WITH MONOTONIC LOADING AT SLOW STRAIN RATES**

**The Basic Equation for Monotonic Compression Loading**

Mander et al. (1984) have proposed a unified stress-strain approach for confined concrete applicable to both circular and rectangular shaped transverse reinforcement. The stress-strain model is illustrated in Fig. 1 and is based on an equation suggested by Popovics (1973). For a slow (quasi-static) strain rate and monotonic loading, the longitudinal compressive concrete stress  $f_c$  is given by

$$f_c = \frac{f'_{cc} x r}{r - 1 + x^r} \dots \dots \dots (3)$$

where  $f'_{cc}$  = compressive strength of confined concrete (defined later).

$$x = \frac{\epsilon_c}{\epsilon_{cc}} \dots \dots \dots (4)$$

where  $\epsilon_c$  = longitudinal compressive concrete strain.

$$\epsilon_{cc} = \epsilon_{co} \left[ 1 + 5 \left( \frac{f'_{cc}}{f'_{co}} - 1 \right) \right] \dots \dots \dots (5)$$

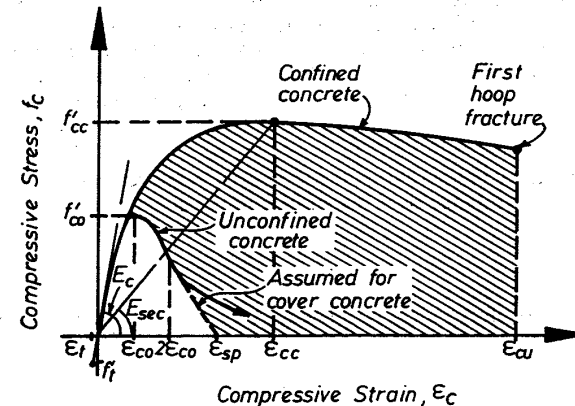


FIG. 1. Stress-Strain Model Proposed for Monotonic Loading of Confined and Unconfined Concrete

as suggested by Richart et al. (1928), where  $f'_{co}$  and  $\epsilon_{co}$  = the unconfined concrete strength and corresponding strain, respectively (generally  $\epsilon_{co} = 0.002$  can be assumed), and

$$r = \frac{E_c}{E_c - E_{sec}} \dots \dots \dots (6)$$

where

$$E_c = 5,000\sqrt{f'_{co}} \text{ MPa} \dots \dots \dots (7)$$

is the tangent modulus of elasticity of the concrete (1 MPa = 145 psi), and

$$E_{sec} = \frac{f'_{cc}}{\epsilon_{cc}} \dots \dots \dots (8)$$

To define the stress-strain behavior of the cover concrete (outside the confined core concrete) the part of the falling branch in the region where  $\epsilon_c > 2\epsilon_{co}$  is assumed to be a straight line which reaches zero stress at the spalling strain,  $\epsilon_{sp}$ .

**Effective Lateral Confining Pressure and the Confinement Effectiveness Coefficient**

An approach similar to the one used by Sheikh and Uzumeri (1980) is adopted to determine the effective lateral confining pressure on the concrete section. The maximum transverse pressure from the confining steel can only be exerted effectively on that part of the concrete core where the confining stress has fully developed due to arching action. Figs. 2 and 3 show the arching action that is assumed to occur between the levels of transverse circular and rectangular hoop reinforcement. Midway between the levels of the transverse reinforcement, the area of ineffectively confined concrete will be largest and the area of effectively confined concrete core  $A_e$  will be smallest.

When using the stress-strain relation, Eq. 3, for computing the strength and ductility of columns it is assumed for convenience that the area of the confined concrete is the area of the concrete within the center lines of the perimeter spiral or hoop,  $A_{cc}$ . In order to allow for the fact that  $A_e < A_{cc}$ , it is considered that the effective lateral confining pressure is

$$f_l = f_l k_e \dots \dots \dots (9)$$

where  $f_l$  = lateral pressure from the transverse reinforcement, assumed to be uniformly distributed over the surface of the concrete core;

$$k_e = \frac{A_e}{A_{cc}} \dots \dots \dots (10)$$

= confinement effectiveness coefficient;  $A_e$  = area of effectively confined concrete core;

$$A_{cc} = A_c(1 - \rho_{cc}) \dots \dots \dots (11)$$

$\rho_{cc}$  = ratio of area of longitudinal reinforcement to area of core of section; and  $A_c$  = area of core of section enclosed by the center lines of the perimeter spiral or hoop.

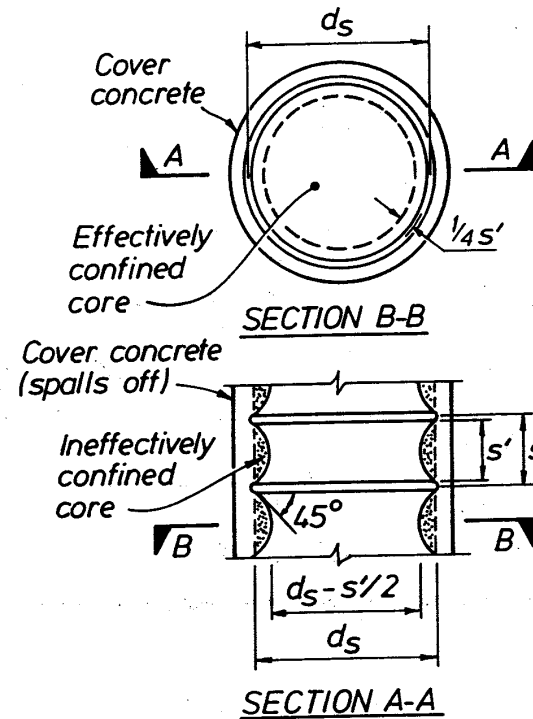


FIG. 2. Effectively Confined Core for Circular Hoop Reinforcement

**Confinement Effectiveness for Sections Confined by Spirals or Circular Hoops**

If in Fig. 2 the arching action is assumed to occur in the form of a second-degree parabola with an initial tangent slope of 45°, the area of an effectively confined concrete core at midway between the levels of transverse reinforcement is

$$A_e = \frac{\pi}{4} \left( d_s - \frac{s'}{2} \right)^2 = \frac{\pi}{4} d_s^2 \left( 1 - \frac{s'}{2d_s} \right)^2 \dots \dots \dots (12)$$

where  $s'$  = clear vertical spacing between spiral or hoop bars; and  $d_s$  = diameter of spiral between bar centers. Also the area of concrete core is

$$A_{cc} = \frac{\pi}{4} d_s^2 (1 - \rho_{cc}) \dots \dots \dots (13)$$

Therefore, from Eq. 10, the confinement effectiveness coefficient is for circular hoops

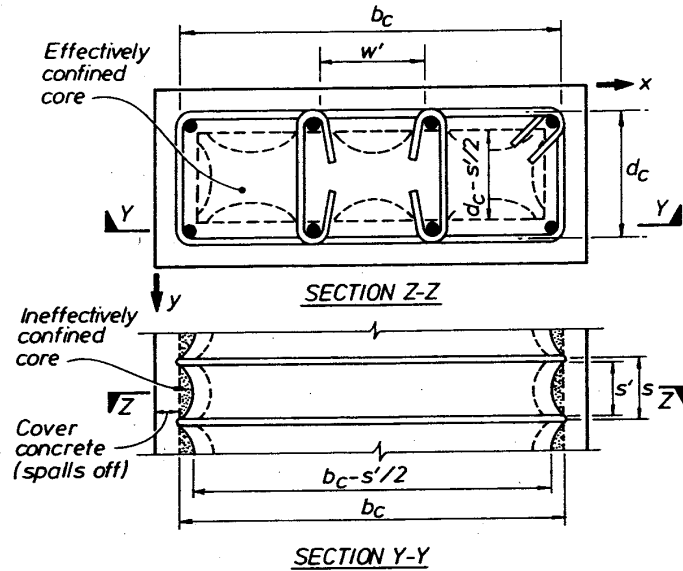


FIG. 3. Effectively Confined Core for Rectangular Hoop Reinforcement

$$k_e = \frac{\left(1 - \frac{s'}{2d_s}\right)^2}{1 - \rho_{cc}} \dots \dots \dots (14)$$

Similarly it can be shown that for circular spirals

$$k_e = \frac{1 - \frac{s'}{2d_s}}{1 - \rho_{cc}} \dots \dots \dots (15)$$

The lateral confining pressure may be found by considering the half body confined by a spiral or circular hoop. If the uniform hoop tension developed by the transverse steel at yield exerts a uniform lateral stress on the concrete core, then equilibrium of forces requires that

$$2f_{yh}A_{sp} = f_l s d_s \dots \dots \dots (16)$$

where  $f_{yh}$  = yield strength of the transverse reinforcement;  $A_{sp}$  = area of transverse reinforcement bar;  $f_l$  = lateral confining pressure on concrete and  $s$  = center to center spacing or pitch of spiral or circular hoop.

Now if  $\rho_s$  = ratio of the volume of transverse confining steel to the volume of confined concrete core, then

$$\rho_s = \frac{A_{sp} \pi d_s}{\frac{\pi}{4} d_s^2 s} = \frac{4A_{sp}}{d_s s} \dots \dots \dots (17)$$

Substituting Eq. 17 into Eq. 16 and rearranging gives

$$f_l = \frac{1}{2} \rho_s f_{yh} \dots \dots \dots (18)$$

Therefore from Eq. 9, the effective lateral confining stress on the concrete is

$$f_l = \frac{1}{2} k_e \rho_s f_{yh} \dots \dots \dots (19)$$

where  $k_e$  is given by Eqs. 14 or 15.

**Confinement Effectiveness for Rectangular Concrete Sections Confined by Rectangular Hoops with or without Cross Ties**

In Fig. 3, the arching action is again assumed to act in the form of second-degree parabolas with an initial tangent slope of 45°. Arching occurs vertically between layers of transverse hoop bars and horizontally between longitudinal bars. The effectively confined area of concrete at hoop level is found by subtracting the area of the parabolas containing the ineffectively confined concrete. For one parabola, the ineffectual area is  $(w_i)^2/6$ , where  $w_i$  is the  $i$ th clear distance between adjacent longitudinal bars (see Fig. 3). Thus the total plan area of ineffectively confined core concrete at the level of the hoops when there are  $n$  longitudinal bars is

$$A_i = \sum_{i=1}^n \frac{(w_i)^2}{6} \dots \dots \dots (20)$$

Incorporating the influence of the ineffective areas in the elevation (Fig. 3), the area of effectively confined concrete core at midway between the levels of transverse hoop reinforcement is

$$A_e = \left(b_c d_c - \sum_{i=1}^n \frac{(w_i)^2}{6}\right) \left(1 - \frac{s'}{2b_c}\right) \left(1 - \frac{s'}{2d_c}\right) \dots \dots \dots (21)$$

where  $b_c$  and  $d_c$  = core dimensions to centerlines of perimeter hoop in  $x$  and  $y$  directions, respectively, where  $b_c \geq d_c$ . Also, the area of concrete core enclosed by the perimeter hoops is given by Eq. 11. Hence from Eq. 10 the confinement effectiveness coefficient is for rectangular hoops

$$k_e = \frac{\left(1 - \sum_{i=1}^n \frac{(w_i)^2}{6b_c d_c}\right) \left(1 - \frac{s'}{2b_c}\right) \left(1 - \frac{s'}{2d_c}\right)}{(1 - \rho_{cc})} \dots \dots \dots (22)$$

It is possible for rectangular reinforced concrete members to have different quantities of transverse confining steel in the  $x$  and  $y$  directions. These may be expressed as

$$\rho_x = \frac{A_{sx}}{s d_c} \dots \dots \dots (23)$$

and

$$\rho_y = \frac{A_{sy}}{sb_c} \dots \dots \dots (24)$$

where  $A_{sx}$  and  $A_{sy}$  = the total area of transverse bars running in the x and y directions, respectively (see Fig. 3).

The lateral confining stress on the concrete (total transverse bar force divided by vertical area of confined concrete) is given in the x direction as

$$f_{lx} = \frac{A_{sx}}{sd_c} f_{yh} = \rho_x f_{yh} \dots \dots \dots (25)$$

and in the y direction as

$$f_{ly} = \frac{A_{sy}}{sb_c} f_{yh} = \rho_y f_{yh} \dots \dots \dots (26)$$

From Eq. 9 the effective lateral confining stresses in the x and y directions are

$$f'_{lx} = k_e \rho_x f_{yh} \dots \dots \dots (27)$$

$$\text{and } f'_{ly} = k_e \rho_y f_{yh} \dots \dots \dots (28)$$

where  $k_e$  is given in Eq. 22.

**Compressive Strength of Confined Concrete,  $f'_{cc}$**

To determine the confined concrete compressive strength  $f'_{cc}$ , a constitutive model involving a specified ultimate strength surface for multiaxial compressive stresses is used in this model. The "five-parameter" multiaxial failure surface described by William and Warnke (1975) is adopted, since it provides excellent agreement with triaxial test data. The calculated ultimate strength surface based on the triaxial tests of Schickert and Winkler (1977) is adopted here. Details of the calculations have been given by Elwi and Murray (1979).

The general solution of the multiaxial failure criterion in terms of the two lateral confining stresses is presented in Fig. 4. When the confined concrete core is placed in triaxial compression with equal effective lateral confining stresses  $f'_i$  from spirals or circular hoops, it can be shown that the confined compressive strength given is:

$$f'_{cc} = f'_{co} \left( -1.254 + 2.254 \sqrt{1 + \frac{7.94 f'_i}{f'_{co}}} - 2 \frac{f'_i}{f'_{co}} \right) \dots \dots \dots (29)$$

where  $f'_{co}$  = unconfined concrete compressive strength; and  $f'_i$  is given by Eq. 19.

As a numerical example, consider a column with an unconfined strength of  $f'_{co} = 30$  MPa (4,350 psi) and confining stresses given by Eqs. 28 and 29 of  $f'_{ly} = 2.7$  MPa (390 psi) and  $f'_{lx} = 5.1$  MPa (740 psi). Then, by following the dotted line in Fig. 4, the compressive strength of the confined concrete is found to be  $f'_{cc} = 1.65 \times 30 = 49.5$  MPa (7,170 psi).

**Monotonic Tensile Loading**

A linear stress-strain relation is assumed in tension up to the tensile strength, provided the tensile strength has not been exceeded. The longitudinal stress  $f_c$  is given by

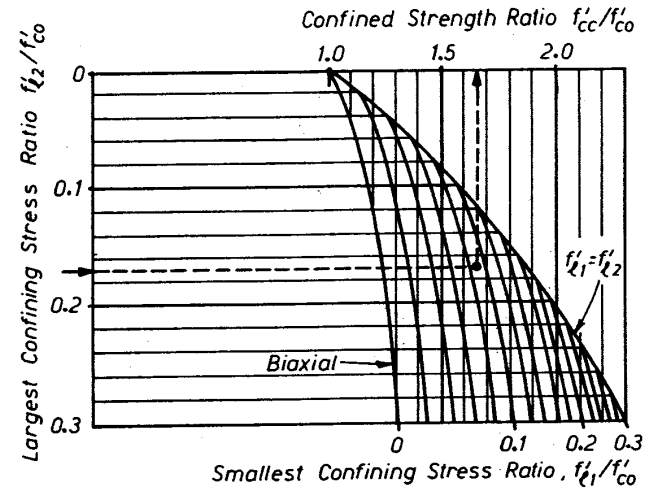


FIG. 4. Confined Strength Determination from Lateral Confining Stresses for Rectangular Sections

$$f_c = E_c \epsilon_c \quad \text{when } f_c < f'_i \dots \dots \dots (30a)$$

otherwise

$$f_c = 0 \dots \dots \dots (30b)$$

where  $E_c$  = tangent modulus of elasticity of concrete given by Eq. 8;  $\epsilon_c$  = longitudinal tensile concrete strain; and  $f'_i$  = tensile strength of concrete.

**STRESS-STRAIN RELATION FOR CYCLIC LOADING AT SLOW STRAIN RATES**

The monotonic loading stress-strain curve is assumed to form an envelope to the cyclic loading stress-strain response. That is, the monotonic curve is assumed to be the skeleton curve. This was found to be the case in two studies by Sinha et al. (1964) and Karsan and Jirsa (1969) for tests on unconfined (plain) concrete specimens. The test results for confined concrete by Mander et al. (1984) shows that this assumption is also reasonable for reinforced concrete specimens.

**Unloading Branches**

Unloading of the concrete may occur from either the compressive or tensile portion of the skeleton stress-strain curve as follows:

**Compression Unloading**

Fig. 5 shows a stress-strain curve including an unloading branch. To establish a reversal stress-strain curve from the compressive loading curve given by Eq. 3, a plastic strain  $\epsilon_{pl}$  based on the coordinate at the reversal point ( $\epsilon_{un}, f_{un}$ ) on unloading needs to be determined. The procedure

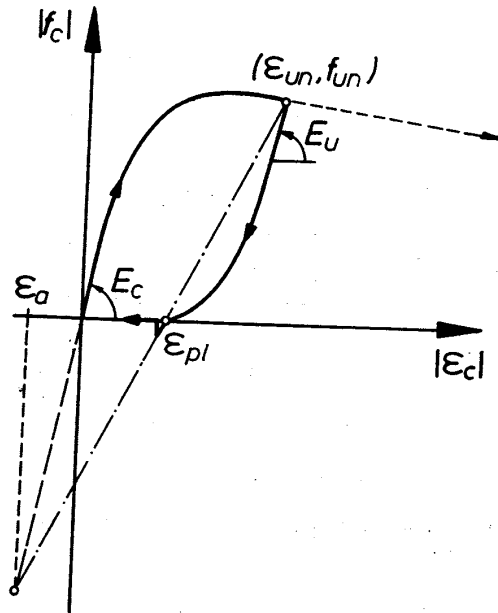


FIG. 5. Stress-Strain Curves for Unloading Branch and Determination of Plastic Strain  $\epsilon_{pl}$  from Common Strain  $\epsilon_a$

adopted here is similar to the approach used by Takiguchi et al. (1976) but modified so that it is suitable for both unconfined and confined concrete. The plastic strain  $\epsilon_{pl}$  lies on the unloading secant slope as shown in Fig. 5, which in turn is dependent on the strain  $\epsilon_a$  at the intersection of the initial tangent and the plastic unloading secant slopes. The strain  $\epsilon_a$  is given by

$$\epsilon_a = a\sqrt{\epsilon_{un}\epsilon_{cc}} \dots \dots \dots (31)$$

Takiguchi et al. (1976) used  $a = 0.1175$  in Eq. 31 for plain concrete. In this investigation, this value for the coefficient  $a$  was found to be unsuitable for both unconfined and confined concrete and was replaced by the greater of

$$a = \frac{\epsilon_{cc}}{\epsilon_{cc} + \epsilon_{un}} \dots \dots \dots (32)$$

or

$$a = \frac{0.09\epsilon_{un}}{\epsilon_{cc}} \dots \dots \dots (33)$$

The plastic strain on the secant line between  $\epsilon_a$  and  $\epsilon_{un}$  is given by

$$\epsilon_{pl} = \epsilon_{un} - \frac{(\epsilon_{un} + \epsilon_a)f_{un}}{(f_{un} + E_c\epsilon_a)} \dots \dots \dots (34)$$

The unloading curve shown in Fig. 5 is then assumed to be defined as a modified form of Eq. 3, namely

$$f_c = f_{un} - \frac{f_{un}xr}{r - 1 + x^r} \dots \dots \dots (35)$$

in which

$$r = \frac{E_u}{E_u - E_{sec}} \dots \dots \dots (36)$$

$$E_{sec} = \frac{f_{un}}{\epsilon_{un} - \epsilon_{pl}} \dots \dots \dots (37)$$

$$x = \frac{\epsilon_c - \epsilon_{un}}{\epsilon_{pl} - \epsilon_{un}} \dots \dots \dots (38)$$

and where  $E_u$  = initial modulus of elasticity at the onset of unloading and is given by

$$E_u = bcE_c \dots \dots \dots (39)$$

where

$$b = \frac{f_{un}}{f'_{co}} \geq 1 \dots \dots \dots (40)$$

$$c = \left(\frac{\epsilon_{cc}}{\epsilon_{un}}\right)^{0.5} \leq 1 \dots \dots \dots (41)$$

The coefficients  $a$ ,  $b$ , and  $c$  in Eqs. 32, 40, and 41 were evaluated by trial and error to give the "best fit" of the assumed stress-strain relation (Eq. 35) to selected experimental unloading curves. The experimental curves used were taken from Karson and Jirsa (1969) and Sinha et al. (1964) for unconfined concrete, and from Mander et al. (1984) for confined reinforced concrete.

If strain reversal occurs from a reloading branch rather than the skeleton curves as assumed, then the current level of plastic strain  $\epsilon_{pl}$  is still used.

*Tensile Unloading*

The effect of preloading in compression on the tension strength of concrete has been investigated by Moria and Kaku (1975). Based on their test results the assumed deterioration in tensile strength due to previous compressive strain histories was idealized as shown in Fig. 6.

On unloading from the compressive branch, the tension strength becomes:

$$f_t = f'_t \left(1 - \frac{\epsilon_{pl}}{\epsilon_{cc}}\right) \dots \dots \dots (42)$$

If  $\epsilon_{pl} < \epsilon_{cc}$  then  $f_t = 0$ . Thus the stress-strain relation becomes

$$f_t = E_t(\epsilon_c - \epsilon_{pl}) \dots \dots \dots (43)$$

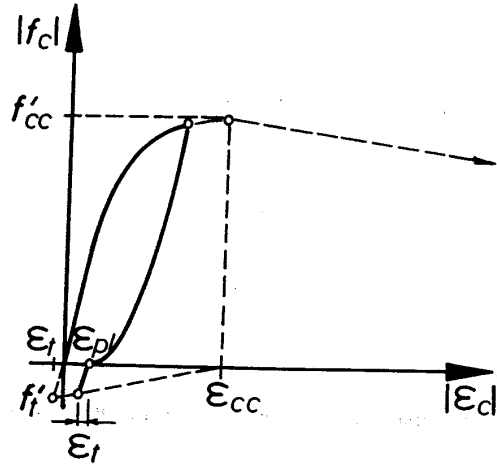


FIG. 6. Assumed Deterioration in Tensile Strength of Concrete due to Prior Compression Loading

where

$$E_t = \frac{f'_t}{\epsilon_t} \dots \dots \dots (44)$$

and

$$\epsilon_t = \frac{f'_t}{E_c} \dots \dots \dots (45)$$

When the tensile strain at the tensile strength is exceeded, i.e.,  $\epsilon_c > (\epsilon_t - \epsilon_{pl})$ , cracks open and the tensile strength of concrete for all subsequent loadings is assumed to be zero.

**Reloading Branches**

Fig. 7 shows the stress-strain curves including unloading and reloading branches. The coordinates of the point of reloading ( $\epsilon_{ro}, f_{ro}$ ) may be from either the unloading curve, or from the cracked state in which  $\epsilon_{ro} = (\epsilon_{pl} - \epsilon_t)$  and  $f_{ro} = 0$ , as shown in Fig. 7. A linear stress-strain relation is assumed between  $\epsilon_{ro}$  and  $\epsilon_{un}$  to a revised stress magnitude to account for cyclic degradation. The new stress point ( $f_{new}$ ) is assumed to be given by the equation

$$f_{new} = 0.92f_{un} + 0.08f_{ro} \dots \dots \dots (46)$$

The same experimental data used to calibrate Eq. 46 was used for Eqs. 32-41.

A parabolic transition curve is used between the linear relation

$$f_c = f_{ro} + E_r(\epsilon_c - \epsilon_{ro}) \dots \dots \dots (47)$$

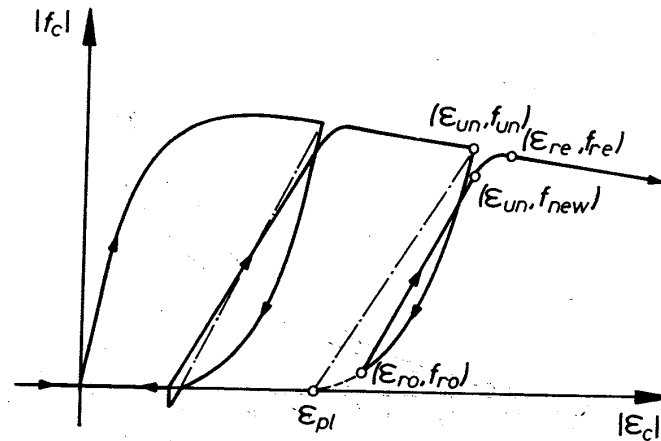


FIG. 7. Stress-Strain Curves for Reloading Branch

where

$$E_r = \frac{f_{ro} - f_{new}}{\epsilon_{ro} - \epsilon_{un}} \dots \dots \dots (48)$$

and the monotonic stress-strain curve (Eq. 3) return coordinate  $(\epsilon_{re}, f_{re})$ . The common return strain ( $\epsilon_{re}$ ) is assumed to be given by the following equation

$$\epsilon_{re} = \epsilon_{un} + \frac{f_{un} - f_{new}}{E_r \left( 2 + \frac{f'_{cc}}{f'_{co}} \right)} \dots \dots \dots (49)$$

where  $E_r$  is given by Eq. 48.

The parabolic transition curve is then described by

$$f_c = f_{re} + E_r x + Ax^2 \dots \dots \dots (50)$$

where

$$x = (\epsilon_c - \epsilon_{re}) \dots \dots \dots (51)$$

$$A = \frac{E_r - E_{re}}{-4[(f_{new} - f_{re}) - E_r(\epsilon_{un} - \epsilon_{re})]} \dots \dots \dots (52)$$

$E_{re}$  and  $f_{re}$  = the common return point tangent modulus and the stress determined from the return strain,  $\epsilon_{re}$ , using the monotonic stress-strain relation (Eq. 3), respectively.

**EFFECT OF RATE OF STRAIN ON STRESS-STRAIN RELATION**

Concrete exhibits a significant increase in both the strength and stiffness when loaded at an increased strain rate. Experimental data on the

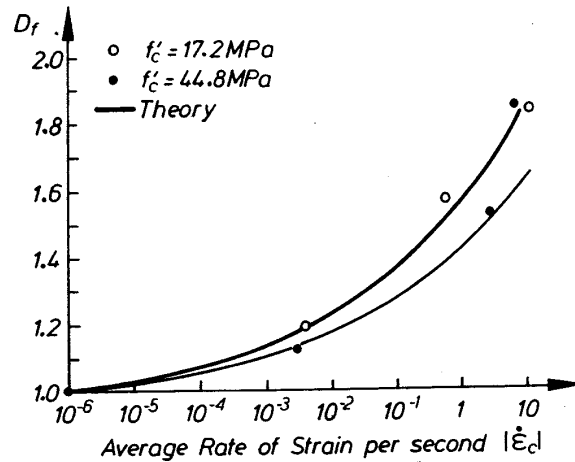


FIG. 8. Dynamic Magnification Factors  $D_f$  to Allow for Strain Rate Effects on Strength

properties of concrete subjected to high strain rates has been reported by Watstein (1953), Bresler and Bertero (1975), Scott et al. (1982), Ahmad and Shah (1985), Dilger et al. (1984), and others.

The stress-strain relations given by Eqs. 3-52 have been written for slow (quasi-static) strain rates. However these equations will also apply to concrete loaded at high strain rates providing that the control parameters  $f'_{co}$ ,  $E_c$ , and  $E_{co}$  of the unconfined concrete are modified so as to apply to the relevant strain rate  $\dot{\epsilon}_c$ .

Relationships for the strain-rate dependence of these parameters, established by Mander et al. (1984) from the experimental results, are as follows.

**Dynamic Strength**

$$(f'_{co})_{dyn} = D_f f'_{co} \dots \dots \dots (53)$$

where  $f'_{co}$  = the quasi-static compressive strength of concrete and

$$D_f = \frac{1 + \left[ \frac{\epsilon_c}{0.035(f'_{co})^2} \right]^{1/6}}{1 + \left[ \frac{0.00001}{0.035(f'_{co})^2} \right]^{1/6}} \dots \dots \dots (54)$$

where  $\epsilon_c$  = rate of strain in  $s^{-1}$ ; and  $f'_{co}$  is in MPa (1 MPa = 145 psi). The dynamic magnification factor  $D_f$  was found by regression analysis of the experimental results of Watstein (1953) on plain concrete specimens of different strengths. Fig. 8 shows a plot of Eq. 54 compared with those experimental results for two concrete strengths. Good agreement was

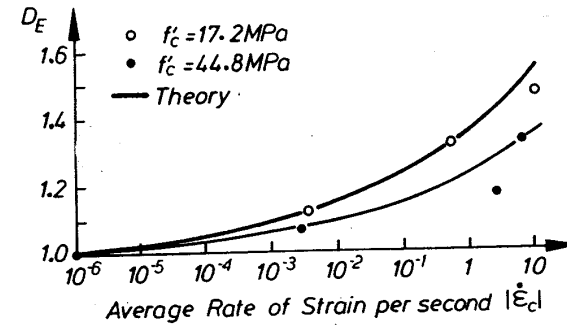


FIG. 9. Dynamic Magnification Factors  $D_E$  to Allow for Strain Rate Effects on Stiffness

provided by the limited data on large concrete specimens tested by the writers.

**Dynamic Stiffness**

$$(E_c)_{dyn} = D_E E_c \dots \dots \dots (55)$$

where  $E_c$  = the quasi-static modulus of elasticity; and

$$D_E = \frac{1 + \left[ \frac{\epsilon_c}{0.035(f'_{co})^3} \right]^{1/6}}{1 + \left[ \frac{0.00001}{0.035(f'_{co})^3} \right]^{1/6}} \dots \dots \dots (56)$$

where  $\epsilon_c$  = rate of strain in  $s^{-1}$ ; and  $f'_{co}$  = the quasi-static compressive strength of concrete in MPa (1 MPa = 145 psi). The dynamic magnification factor  $D_E$  was found by regression analysis of the experimental results of Watstein (1953). Fig. 9 shows a plot of Eq. 56 compared with those results for two concrete strengths.

**Dynamic Strain at Peak Stress**

$$(\epsilon_{co})_{dyn} = D_\epsilon \epsilon_{co} \dots \dots \dots (57)$$

where  $\epsilon_{co}$  = quasi-static strain at peak stress; and

$$D_\epsilon = \frac{1}{3D_f} \left( 1 + \sqrt{1 + \frac{3D_f^2}{D_E}} \right) \dots \dots \dots (58)$$

The results of experiments by various investigators appear to show no consensus on the value of the strain at peak stress for high rates of strain. Eq. 58 was derived assuming that the work done on concrete to achieve its strength is constant, irrespective of the rate of strain. Generally good agreement is obtained with most observed results.



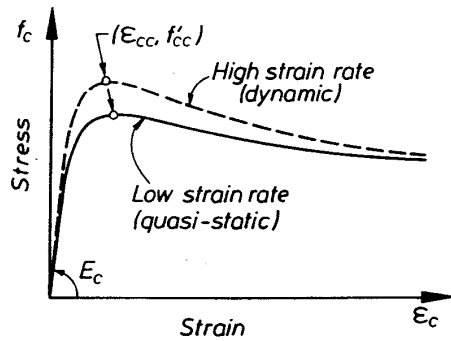


FIG. 10. Effect of Strain Rate on Monotonic Stress-Strain Relation for Concrete

Fig. 10 shows the typical results obtained from the application of Eqs. 53–58 to predict the stress-strain curve of concrete at high and low strain rates. It will be seen that an increase in the strain rate results in an increase in the strength  $f'_{cc}$  and the initial stiffness  $E_c$ , and a decrease in the strain at peak stress  $\epsilon_{cc}$ . There is also an increase in the steepness of the falling branch curve, such that the dynamic curve approaches the quasi-static curve at high strains.

As an example of the influence of Eqs. 53–58, consider concrete of unconfined strength  $f'_{co} = 30$  MPa (4,350 psi) tested at a strain rate of 1%/sec. Eqs. 53 and 54 predict a strength increase of 27%, Eqs. 55 and 56 predict an initial stiffness increase also of 27%, and Eqs. 57 and 58 predict a reduction in strain at peak stress of 13%.

**ULTIMATE CONCRETE COMPRESSION STRAIN**

In order to calculate the available ultimate rotation capacity at a plastic hinge in a reinforced concrete flexural member, it is necessary to be able to predict the ultimate concrete compressive strain  $\epsilon_{cu}$ . Early experimental work on the deformability of compressed concrete in reinforced concrete members by a number of investigators resulted in the development of several empirical equations for  $\epsilon_{cu}$ . A summary of some of those early equations for  $\epsilon_{cu}$  is given in Park and Paulay (1975).

Recently Scott et al. (1982) have proposed that the ultimate concrete compressive strain be defined as the longitudinal strain at which the first hoop fracture occurs, since that strain can be regarded as the end of the useful region of the stress-strain curve for the confined concrete core. After first hoop fracture there is a sudden drop in the compression load capacity of the core concrete due to reduction in confinement, and there is also a loss of buckling restraint for the compressed longitudinal bars.

Subsequently, Mander et al. (1984) proposed a rational method for predicting the longitudinal concrete compressive strain at first hoop fracture based on an energy balance approach. In this approach, the additional ductility available when concrete members are confined is considered to be due to the energy stored in the transverse reinforcement.

Consider the stress-strain curves for unconfined and confined concrete shown in Fig. 1. The area under each curve represents the total strain energy per unit volume required to “fail” the concrete. The increase in strain energy at failure resulting from confinement (shown shaded in Fig. 1) can only be provided by the strain energy capacity of the confining reinforcement as it yields in tension. By equating the ultimate strain energy capacity of the confining reinforcement per unit volume of concrete core ( $U_{sh}$ ) to the difference in area between the confined ( $U_{cc}$ ) and the unconfined ( $U_{co}$ ) concrete stress-strain curves, plus additional energy required to maintain yield in the longitudinal steel in compression ( $U_{sc}$ ), the longitudinal concrete compressive strain corresponding to hoop fracture can be calculated. Thus

$$U_{sh} = U_{cc} + U_{sc} - U_{co} \dots \dots \dots (59)$$

Substituting in Eq. 59 gives

$$\rho_s A_{cc} \cdot \int_0^{\epsilon_{sf}} f_s d\epsilon_s = A_{cc} \cdot \int_0^{\epsilon_{cu}} f_c d\epsilon_c + \rho_{cc} A_{cc} \cdot \int_0^{\epsilon_{cu}} f_{sf} d\epsilon_c - A_{cc} \cdot \int_0^{\epsilon_{sp}} f_c d\epsilon_c \dots \dots (60)$$

where  $\rho_s$  = ratio of volume of transverse reinforcement to volume of concrete core;  $A_{cc}$  = area of concrete core,  $f_s$  and  $\epsilon_s$  = stress and strain in transverse reinforcement;  $\epsilon_{sf}$  = fracture strain of transverse reinforcement;  $f_c$  and  $\epsilon_c$  = longitudinal compressive stress and strain in concrete;  $\epsilon_{cu}$  = ultimate longitudinal concrete compressive strain;  $\rho_{cc}$  = ratio of volume of longitudinal reinforcement to volume of concrete core,  $f_{sf}$  = stress in longitudinal reinforcement; and  $\epsilon_{sp}$  = spalling strain of unconfined concrete.

In the first term on the left-hand side of Eq. 60, the expression

$$\int_0^{\epsilon_{sf}} f_s d\epsilon_s = U_{sf} \dots \dots \dots (61)$$

is the total area under the stress-strain curve for the transverse reinforcement up to the fracture strain  $\epsilon_{sf}$ . Results from tests carried out by Mander et al. (1984) in New Zealand on grade 275 ( $f_y \geq 40$  ksi) and grade 380 ( $f_y \geq 55$  ksi) reinforcement of various bar diameters indicates that  $U_{sf}$  is effectively independent of bar size or yield strength, and may be taken (within  $\pm 10\%$ ) as

$$U_{sf} = 110 \text{ MJ/m}^3 \dots \dots \dots (62)$$

For this steel  $\epsilon_{sf}$  ranged between 0.24 and 0.29.

For the last term on the right-hand side of Eq. 60, the area under the stress-strain curve for unconfined concrete is required. It was found from analyses of measured data from a range of plain concrete specimens that the area under the stress-strain curve for unconfined concrete may be approximated as

$$\int_0^{\epsilon_{sp}} f_c d\epsilon_c = 0.017 \sqrt{f'_{co}} \text{ MJ/m}^3 \dots \dots \dots (63)$$

$\epsilon f'_{co}$  = quasi-static compressive strength of concrete in MPa (1 MPa = 145 psi).

Thus Eq. 61 simplifies to

$$110\rho_s = \int_0^{\epsilon_{cu}} f_c d\epsilon_c + \int_0^{\epsilon_{cu}} f_{sl} d\epsilon_c - 0.017\sqrt{f'_{co}} MJ/m^3 \dots \dots \dots (64)$$

With a knowledge of  $f_c$  from Eq. 3 and  $f_{sl}$  as a function of longitudinal strain, the longitudinal concrete compressive strain  $\epsilon_{cu}$  at the stage of first fracture of the transverse reinforcement can be solved for numerically using Eq. 64.

**CONCLUSIONS**

The development of the analytical stress-strain model for confined concrete leads to the following conclusions:

1. Reinforced concrete members with axial compression forces may be confined by using transverse steel to enhance the member strength and ductility. For a particular transverse reinforcement configuration the effective confining stresses  $f'_{lx}$  and  $f'_{ly}$  in the x and y directions can be calculated from the transverse reinforcement and a confinement effectiveness coefficient  $k_e$  which defines the effectively confined concrete core area by taking into account the arching action that occurs between the transverse hoops and between longitudinal bars.
2. A "five-Parameter" maximum strength criterion uses the effective confining stresses to determine the confined concrete strength  $f'_{cc}$  on the ultimate strength surface. The increase in the strain at ultimate strength  $\epsilon_{cc}$  is assumed to be about five times the strength increase.
3. The form of the stress-strain curve for confined concrete can be expressed in terms of a simple uniaxial relation suggested by Popovics and only requires three control parameters ( $f'_{cc}$ ,  $\epsilon_{cc}$ , and  $E_c$ ). Unloading and reloading curves can be developed for cyclic loading response.
4. An allowance for the dynamic response in stress-strain modelling may be incorporated by modifying the quasi-static concrete parameters ( $f'_{cc}$ ,  $\epsilon_{cc}$ , and  $E_c$ ) by dynamic magnification factors which are subsequently used in the stress-strain model.
5. The ultimate concrete compressive strain of a section, defined as that strain at which first hoop fracture occurs, may be determined by tracing the work done on the confined concrete and longitudinal steel when deformed in compression. In this energy balance approach, when the work done exceeds the available strain energy of the transverse steel, then hoop fracture occurs and the section can be considered to have reached its ultimate deformation.
6. The usefulness of the model presented herein will become apparent when compared with the observed behavior of confined reinforcement concrete members under dynamic cyclic loading. Such studies are reported in a companion paper (Mander et al. 1988).

**ACKNOWLEDGMENTS**

The work described in this paper was conducted by Dr. J. B. Mander as part of his Ph.D. studies at the University of Canterbury under the

supervision of Prof. M. J. N. Priestley and Prof. R. Park. The financial assistance provided by the University of Canterbury, New Zealand Railways Corporation and the New Zealand National Roads Board is gratefully acknowledged.

**APPENDIX I. REFERENCES**

Ahmad, S. M., and Shah, S. P. (1982). "Stress-strain curves of concrete confined by spiral reinforcement." *Am. Concr. Inst. J.*, 79(6), 484-490.

Ahmad, S. M., and Shah, S. P. (1985). "Behavior of hoop confined concrete under high strain rates." *Am. Concr. Inst. J.*, 82(5), 634-647.

Balmer, G. G. (1944). "Shearing strength of concrete under high triaxial stress—computation of Mohr's envelope as a curve." *SP-23, Structural Research Laboratory, U.S. Bureau of Reclamation.*

Bazant, Z. P., and Bhat, P. D. (1976). "Endochronic theory of inelasticity and failure of concrete." *J. Engrg. Mech. Div.*, ASCE, 102(4), 701-722.

Bazant, Z. P., and Bhat, P. D. (1977). "Prediction of hysteresis of reinforced concrete members." *J. Struct. Div.*, ASCE, 103(1), 153-167.

Bresler, B., and Bertero, V. V. (1975). "Influence of high strain rate and cyclic loading on behavior of unconfined and confined concrete in compression." *Proc. 2nd Can. Conf. on Earthquake Engrg.*, McMaster Univ., 1-32.

Desayi, P., Iyengar, K. T. S. A., and Reddy, T. S. (1978). "Equations for stress-strain curve of concrete confined in circular steel spiral." *Mater. and Struct., Res. and Testing*, Paris, France 11(65), 339-345.

Dilger, W. H., Koch, R., and Kowalczyk, (1984). "Ductility of plain and confined concrete under different strain rates." *Am. Concr. Inst. J.*, 81(1), 73-81.

Elwi, A. A., and Murray, D. W. (1979). "A 3D hypoelastic concrete constitutive relationship." *J. Engrg. Mech. Div.*, ASCE, 105(4), 623-641.

Karson, I. D., and Jirsa, J. O. (1969). "Behavior of concrete under compressive loadings." *J. Struct. Engrg. Div.*, ASCE 95(12), 2543-2563.

Kent, D. C., and Park, R. (1971). "Flexural members with confined concrete." *J. Struct. Div.*, ASCE, 97(7), 1969-1990.

Mander, J. B., Priestley, M. J. N., and Park, R. (1984). "Seismic design of bridge piers." *Research Report No. 84-2*, Univ. of Canterbury, New Zealand.

Mander, J. B., Priestley, M. J. N., and Park, R. (1988). "Observed stress-strain behavior of confined concrete." *J. Struct. Engrg.*, ASCE, 114(8), 1827-1849.

Morita, S., and Kaku, T. (1975). "Cracking and deformation of reinforced concrete beams subjected to tension." *Liege Colloquium Inter-Association.*

Park, R., and Leslie, P. D. (1977). "Curvature ductility of circular reinforced concrete columns confined by the ACI spiral." *6th Australasian Conf. on the Mech. of Struct. and Mater.*, vol. 1, 342-349.

Park, R., and Paulay, T. (1975). *Reinforced concrete structures*. John Wiley and Sons, New York, N.Y.

Park, R., Priestley, M. J. N., and Gill, W. D. (1982). "Ductility of square-confined concrete columns." *J. Struct. Div.*, ASCE, 108(4), 929-950.

Popovics, S. (1973). "A numerical approach to the complete stress-strain curves for concrete." *Cement and Concr. Res.*, 3(5), 583-599.

Richart, F. E., Brandtzaeg, A., and Brown, R. L. (1928). "A study of the failure of concrete under confined compressive stresses." *Bulletin 185*, Univ. of Illinois Engineering Experimental Station, Champaign, Ill.

Richart, F. E., Brandtzaeg, A., and Brown, R. L. (1929). "The failure of plain and spirally reinforced concrete in compression." *Bulletin 190*, Univ. of Illinois Engineering Experimental Station, Champaign, Ill.

Roy, H. E. H., and Sozen, M. A. (1964). "Ductility of concrete." *Proc. Int. Symp. on the Flexural Mech. of Reinforced Concrete*, ASCE-American Concrete Institute, 213-224.

Schickert, G., and Winkler, H. (1979). "Results of tests concerning strength and strain of concrete subjected to multiaxial compressive stresses." *Deutscher Ausschuss fur Stahlbeton*, Heft 277, Berlin, West Germany.

Scott, B. D., Park, R., and Priestley, M. J. N. (1982). "Stress-strain behavior of concrete confined by overlapping hoops at low and high strain rates." *Am. Concr. Inst. J.*, 79(1), 13-27.

Sheikh, S. A., and Uzumeri, S. M. (1980). "Strength and ductility of tied concrete columns." *J. Struct. Div.*, A.S.C.E., 106(5), 1079-1102.

Sinha, B. P., Gerstle, K. H., and Tulin, L. G. (1964). "Stress-strain relation for concrete under cyclic loading." *Am. Concr. Inst. J.*, 61(2), 195-211.

Takiguchi, K., et al. (1976). "Analysis of reinforced concrete sections subjected to biaxial bending moments." *Trans.*, Architectural Institute of Japan, 250, 1-8.

Vellenas, J., Bertero, V. V., and Popov, E. P. (1977). "Concrete confined by rectangular hoops subjected to axial loads." *Report 77/13*, Earthquake Engineering Research Center, Univ. of California, Berkeley, Calif.

Watstein, D. (1953). "Effect of straining rate on the compressive strength and elastic properties of concrete." *Am. Concr. Inst. J.*, 24(8), 729-744.

William, K. J., and Warnke, E. P. (1975). "Constitutive model for the triaxial behavior of concrete." *Proc.*, International Association for Bridge and Structural Engineering, vol. 19, 1-30.

Zahn, F. A., Park, R., and Priestley, M. J. N. (1986). "Design of reinforced concrete bridge columns for strength and ductility." *Research Report 86-7*, Univ. of Canterbury, Christchurch, New Zealand.

**APPENDIX II. NOTATION**

The following symbols are used in this paper:

- $A_c$  = area of core of section within center lines of perimeter spiral;
- $A_{cc}$  = area of core within center lines of perimeter spiral or hoops excluding area of longitudinal steel;
- $A_e$  = area of effectively confined core concrete;
- $A_i$  = total area of ineffectively confined core concrete at the level of hoops;
- $A_{sp}$  = area of spiral bar;
- $A_{sx}$  = total area of transverse reinforcement parallel to x-axis;
- $A_{sy}$  = total area of transverse reinforcement parallel to y-axis;
- $b_c$  = concrete core dimension to center line of perimeter hoop in x-direction;
- $D_E$  = dynamic magnification factor for initial modulus of elasticity for concrete due to dynamic loading;
- $D_f$  = dynamic magnification factor for concrete strength due to dynamic loading;
- $D_e$  = dynamic magnification factor for strain at peak stress due to dynamic loading;
- $d_c$  = concrete core dimension to center line of perimeter hoop in y direction;
- $d_s$  = diameter of spiral;
- $E_c$  = modulus of elasticity of concrete;
- $E_{re}$  = return point modulus of elasticity on monotonic stress-strain curve for concrete;
- $E_{sec}$  = secant modulus of confined concrete at peak stress;
- $E_u$  = initial concrete modulus of elasticity at onset of unloading;
- $f_c$  = longitudinal concrete stress;
- $f'_{cc}$  = compressive strength (peak stress) of confined concrete;

- $f'_{co}$  = compressive strength of unconfined concrete;
- $(f'_{co})_{dyn}$  = dynamic compressive strength of unconfined concrete;
- $f_i$  = lateral confining stress on concrete from transverse reinforcement;
- $f_l$  = effective lateral confining stress;
- $f_{lx}$  = lateral confining stress on concrete in x direction;
- $f'_{lx}$  = effective lateral confining stress in x direction;
- $f_{ly}$  = lateral confining stress on concrete in y direction;
- $f'_{ly}$  = effective lateral confining stress in y direction;
- $f'_{l1}$  = smaller confining stress;
- $f'_{l2}$  = larger confining stress;
- $f_{new}$  = new concrete stress on reloading at strain of  $\epsilon_{un}$ ;
- $f_{re}$  = return point stress on monotonic stress-strain curve;
- $f_{ro}$  = concrete stress at reloading reversal;
- $f_s$  = steel stress;
- $f_{sl}$  = stress in longitudinal steel reinforcement;
- $f'_t$  = modified tensile strength of concrete due to cyclic loading;
- $f'_t$  = tensile strength of concrete;
- $f_{un}$  = reversal (unloading) stress in concrete model;
- $f_y$  = yield stress of steel;
- $f_{yh}$  = yield strength of transverse reinforcement;
- $h$  = member overall depth;
- $k_e$  = confinement effectiveness coefficient;
- $k_1, k_2$  = concrete strength and strain enhancement coefficients;
- $s$  = spiral spacing or pitch;
- $s'$  = clear spacing between spiral or hoop bars;
- $U_{cc}$  = strain energy stored by confined concrete per unit volume;
- $U_{co}$  = strain energy stored by unconfined concrete per unit volume;
- $U_{sc}$  = strain energy stored by longitudinal reinforcing steel in compression per unit volume of concrete core;
- $U_{sf}$  = area beneath stress-strain curve for steel from zero load to fracture;
- $U_{sh}$  = strain energy capacity of transverse confining steel per unit volume of concrete core;
- $w$  = spacing of longitudinal bars in rectangular section;
- $w'_i$  =  $i$ th clear transverse spacing between adjacent longitudinal bars;
- $\epsilon_a$  = common strain at intersection of initial tangent and plastic unloading slopes;
- $\epsilon_c$  = longitudinal concrete strain;
- $\epsilon_{cc}$  = strain at maximum concrete stress  $f'_{cc}$ ;
- $\epsilon_{co}$  = strain at maximum stress  $f'_{co}$  of unconfined concrete;
- $\epsilon_{cu}$  = ultimate concrete compressive strain, defined as strain at first hoop fracture;
- $\epsilon_{pl}$  = plastic strain in concrete model;
- $\epsilon_{re}$  = return point strain on monotonic stress-strain curve;
- $\epsilon_{ro}$  = concrete strain at reloading reversal;
- $\epsilon_s$  = steel strain;
- $\epsilon_{sf}$  = tensile fracture strain of steel;